



Incorporation of gold nanoparticles into pH responsive mixed microgel systems

Azwan Mat Lazim^{1*}, Julian Eastoe² and Melanie Bradley²

¹School of Chemical Sciences and Food Technology, Faculty of Science and Technology, Universiti Kebangsaan Malaysia, 43600 Bangi, Selangor, Malaysia

²School of Chemistry, University of Bristol, Bristol BS8 1TS, U.K.

Abstract: Abstract: This research attempts to demonstrate that gold nanoparticles are stable and easily dispersed in mixed microgel systems. In order to prepare stable and controllable responsive systems, the polymers were chosen to be pH responsive. As a result, that the charge signs (+/-) and level could be readily manipulated by adjusting the background solution pH. A switchable 'on' and 'off' system was obtained where these composite AuMES-NP-MM systems switched from a dispersed (pH 10) to a collapsed state (pH 3). This variation in pH affected the dispersion stability due to differences in the microgel particle charges. These systems are therefore successful multifunctional systems which act as reversible scaffolds for support and entrapment of AuMES-NPs. A stability graph was plotted and based on calculation, the amount of AuNPs dispersed in the microgel were estimated. These promising results offer wide applications in various areas especially using the microgel systems as a responsive template.

Keywords: nanoparticles, microgels, dispersion, gold, controllable.

Introduction

Gold colloids have attracted attention for many years¹ and recently there has been received interest with the observation that colloidal gold can acts as a catalyst for many reactions^{2,3}. Initially gold catalysts were used for completing CO oxidation, however, to date, there have been numerous applications added. The catalytic gold is used to produce chemicals such as glyoxalic acid from glyoxal⁴, glyceric acid from glycerol⁵, gluconic acid from glucose⁶, hydrogen peroxide from H₂ and O₂^{7,8}, and a series of aldehydes from alcohols^{8,9}. Thus as a highly demanded metal, alternative handling and processing methods should be explored based on the 3R concept; reduce, reuse and recycle.

Gold nanoparticles (AuNPs) complexes with responsive polymers have inspired for new dimension of research due to their special quality and their broad applications. Employing the responsive polymers allow the potential control of AuNPs characteristics and properties by manipulating the polymer molecular structure, size and composition⁹⁻¹². Interestingly these

*Corresponding author: Azwan Mat Lazim

E-mail address: azwani79@ukm.my

DOI: <http://dx.doi.org/10.13171/mjc.1.5.2012.11.04.19>

responsive polymers are also permitting fully utilization of both organic and aqueous dispersing media. Up to present, various metals including AuNPs have been incorporated and stabilised with responsive polymer and one of them is microgel. Generally, there are two approaches to prepare nanoparticles-microgels composites. The first method involves metal nanoparticles loading into the microgel systems using preform inorganic particles. Whereas the second method, metal nanoparticles are grown in situ within the microgels¹³⁻¹⁵.

Regarding to the synthesis process, the majority of these studies were limited to single-component system. On the other hand, less attention was given to multi-component systems. These mixed-microgel systems (MMS) not only offer various applications but also interesting from a fundamental point of view^{16,17}. Colloidal systems which made from a mixture of anionic and cationic particles can be modified to meet certain requirements. Heteroaggregation occurs when there is an attractive interaction between the different particles of a mixed dispersion, which is at least as strong as the attraction between particles of the same type. According to Islam *et. al.*⁸ an ideal heteroaggregate structure forms when there is only an attractive interaction between different particle types. This is most frequently achieved by mixing dispersions of particles with opposite charges. Reviews which discussed in detail the theoretical background of MMS can be found elsewhere.

The majority of literature describing MGs and MNPs has focused on PNIPAM-based homopolymer microgels e.g.^{6,18-20}. On the other hand, no literature was found describing mixed heteropolymer +/- MGs in combination with MNPs. Interestingly, systems made from a mixture of anionic and cationic particles can be modified to meet certain requirements. The aim of this current work is to demonstrate preparation and applications of systems combining AuNPs with MGs, using commonly available polymers PNIPAM (MG⁻) and PNIPAM-co-poly(2-vinylpyridine) (MG⁺).

This research explores the stability of mixtures of cationic co-polymer and anionic homopolymer microgels with AuNPs for pH-controlled dispersion and separation of the inorganic/organic composites. In this work pH-sensitive mixed-microgel systems are made with mixtures of anionic MG⁻ and a cationic MG⁺ copolymer.. High stability AuNPs have been synthesized as previously reported with 2-mercaptoethanesulfonate (MES) as the stabilizing agent²⁰

Results and Discussion

Gold nanoparticle characterization

Figure 1 shows an electrochromophoretic mobility graph of AuMES-NPs as a function of pH, with 1 mM KCl solution as the background solvent. It is clearly shown that for AuMES-NP dispersions, both electrophoretic mobility and charge remain negative across the entire pH range tested. This is consistent with previous studies¹⁴⁻¹⁶, showing that MES acts as an efficient surface stabilizer for AuMES-NPs, conferring a stable negative surface that is quite resistant to pH.

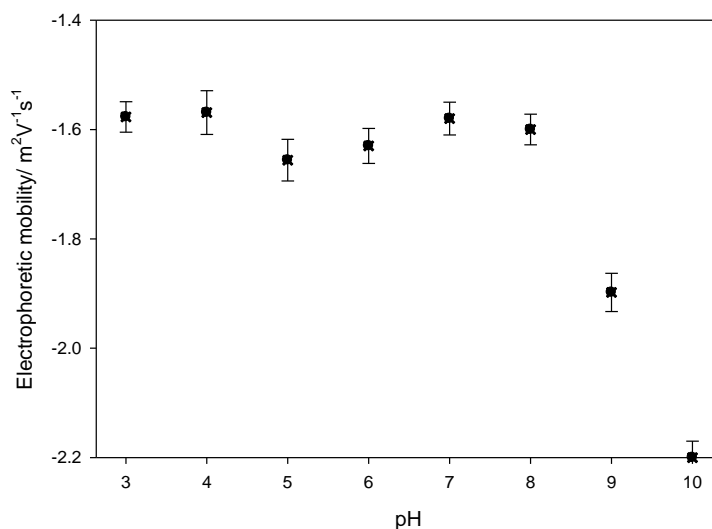


Figure 1:Electrophoretic mobility of AuMES-NP dispersions as a function of pH, from PALS.

UV-Visible spectroscopy

Figure 2 shows the UV spectrum measured for MES-stabilized gold sol at an initial pH of 8 and after the pH has been adjusted to values of 3 and 10. The results showed a typical absorbance profile as was obtained for small particles, owing to Mie Scattering as previously reported¹⁴. Conveniently, the spectral properties of Au-NPs are sensitive to changes in particle size/aggregation, and in particular the position of λ_{max} and the peak width are very sensitive to increases in effective particle size owing to colloidal gold association and aggregation¹⁶. The visible absorption spectrum of the gold solution displays a well defined peak with a maximum at approximately $\lambda_{\text{max}} = 528$ nm, which is consistent with Au-NPs in the size range 5–10 nm, as studied previously^{10,14,16}.

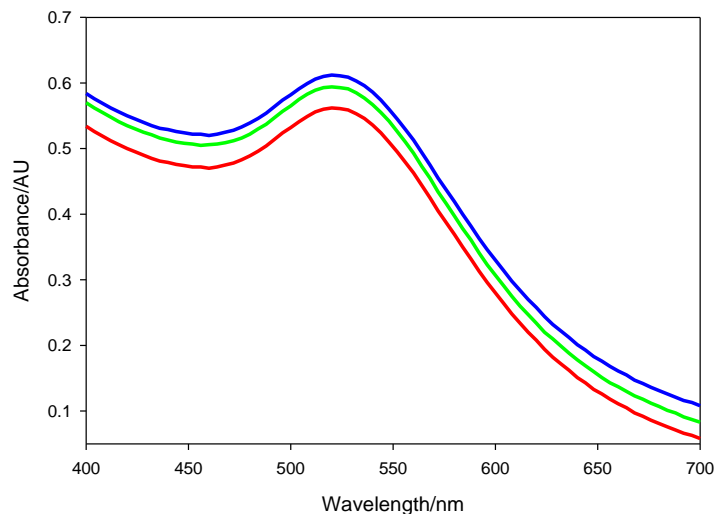


Figure 2:UV-visible spectrum of AuMES-NPs at different pH; 8 (blue), 10 (green), 3 (red).

TEM images

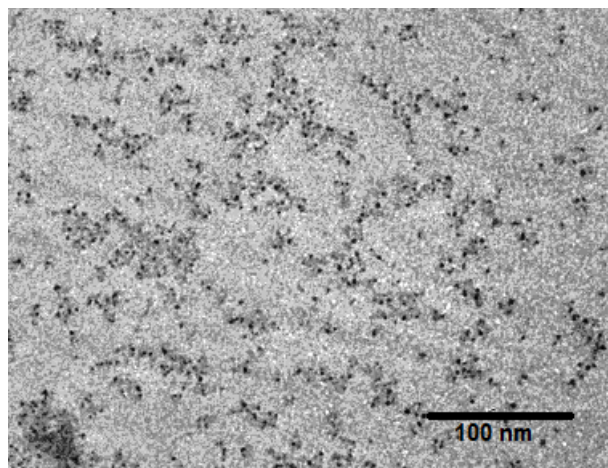


Figure 3: TEM image of AuMES-NPs.

The high resolution image of the AuMES-NPs shown in Figure 3 verifies the existence of small, spherical and relatively polydisperse gold nanoparticles. The average diameter is 7.0 ± 3.0 nm, which is in agreement with UV-visible data reported in the previous section. The existence of large nanoparticles was also observed, possibly an artefact from the grid preparation method¹⁵.

Microgel and nanoparticle characterization

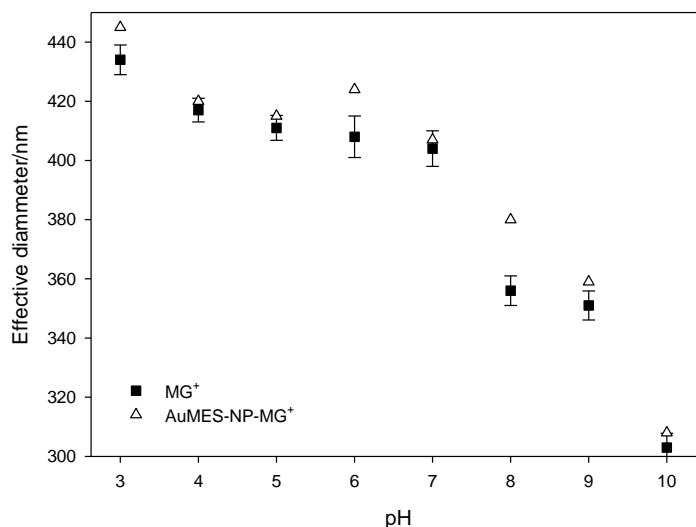


Figure 4: Hydrodynamic diameter of MG⁺ (■) and AuMES-NP-MG⁺ (Δ) systems as a function of pH at 20 °C.

The dependence of apparent hydrodynamic diameter of MG⁺ and AuMES-NP-MG⁺ microgels on pH is shown in Figure 4. On decreasing pH MG⁺ increases in apparent hydrodynamic diameter, i.e. the microgel particles swell due to protonation of 2VP groups in the copolymer

network, resulting in an increase in electrostatic repulsion and osmotic pressure within the particles. As a result of the hydrophilic nature of MG^+ , swelling begins when the pH is a couple of units above the pK_a value of 2VP (approximately 5) and shows a gradual swelling profile with decreasing pH²². The hydrodynamic diameter profile for AuMES-NP- MG^+ is comparable to MG^+ , suggesting that AuMES-NPs do not infiltrate into the microgel network, which would be shown by a decrease in hydrodynamic diameter particularly at low pH where MG^+ are fully swollen and have maximum charge²⁰. Instead AuMES-NPs are most likely to be adsorbed to the surface of the microgel particles.

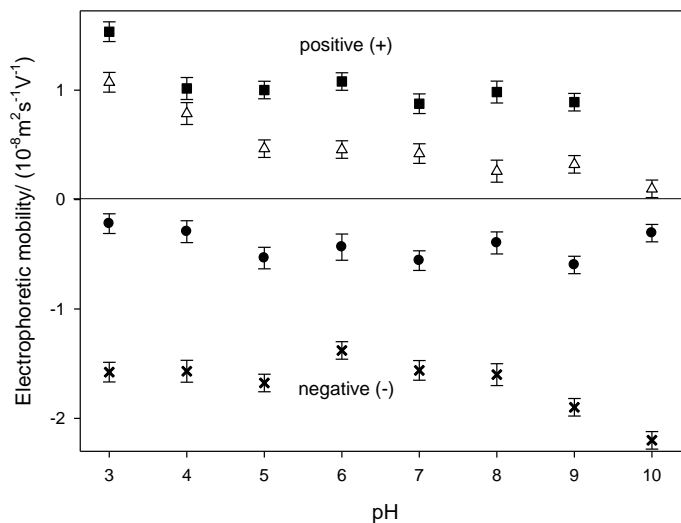


Figure 5: The dependence of electrophoretic mobility on pH for MG^+ (■), AuMES-NP- MG^+ (Δ), MG^- (●) and AuMES-NP (X).

In Figure 5, the electrophoretic mobility (μ_e) of MG^+ , AuMES-NP- MG^+ , MG^- and AuMES-NP particles are shown as a function of pH at 20 °C. For MG^- the values of μ_e remain approximately constant from pH 3 to 9. The magnitude of this mobility decreases as the absolute charge density decreases, which will occur above the pK_a of the pyridine groups; the residual charge at neutral pH is due to the amidine based initiator groups used during free radical polymerization. Similarly MG^- showed negative μ_e across the pH range, owing to the sulfate groups originating from the initiator^{20,21}. Moving now to pure AuMES-NP dispersions, the electrophoretic mobility and charge remains relatively constant and negative over the pH range 3-10. This is consistent with previous studies²⁰, showing that MES is an efficient stabilizer for AuNPs with the surface stabilizing sulfonate groups resilient to pH changes in this range.

The particulate dispersions are individually stable to pH changes. From the observation results, the three separate systems are steadily dispersed as single component without any separation within a month, which indicate that the sample is stable. Thus the mixed negative AuMES-NPs and cationic MGs in the ratio of 2:1 (Table 2) will produce the adsorption of AuMES-NP onto MG^+ , through electrostatic attractions, to form AuMES-NP- MG^+ composites. The infusion of AuMES-NP onto MG^+ will neutralised some of the positive charge. Nevertheless, AuMES-NP- MG^+ composites will still display net positive μ_e values between pH 3 and 10 upon the ratio of mixing as indicated earlier²⁰⁻²³.

The obvious positive charge will decline with the heighten pH, even though AuMES-NP-MG⁺ composite particles remain stably dispersed. Due to unique properties of microgels, there are two causes for this to happen. Firstly, at 25 °C MG⁺ which also comprise of PNIPAM will be swollen with water and also due to the low Hamaker constant effects²². Secondly, MG⁺ has steric some stability at low surface potentials since it is a *soft* hairy particle²³.

MM dispersions preparation

Heteroaggregation behavior for each sample is clearly influenced by the different concentration of oppositely charged microgels, as described in detail by Snowden *et. al.*¹¹. Based on that approach¹¹, MM samples were prepared with varying concentrations, dispersion compositions, and mixed microgel ratios (Table 1).

Hence a large matrix of samples was screened, varying all composition parameters over certain appropriate ranges. In this section five most significant samples from that array were discussed (Table 1) in comparison between results obtained from the samples prepared by author (A-E) and previously reported by Snowden *et.al.*¹¹. In order to determine the systems stability, the authors used three different parameters; temperature, different electrolyte concentrations and pH.

However, among of these parameters the first two parameters were difficult to be controlled and maintained compared to pH. Whereas, Stark *et. al.* has successfully demonstrated that a reversible mixed microgel system was easily controlled owing to pH adjustments. Prior to this convincing results therefore, all samples were examined based on their aggregation as a function of pH at different mass concentration microgels used. The physical state of all samples was determined visually at room temperature. The results obtained showed a significant agreement with the results previously reported¹¹, (for example look at sample A and X, also in sample E and Z). Based on these results a stability diagram was plotted (Figure 6).

Table 1: The composition of samples were studied and the corresponding observations of stability as a function of pH at 25 C, were denoted by stable (S) and unstable (U). In comparison, the results reported by Snowden *et.al*¹¹ shown in the bottom half of the table.

Sample	MG ⁻ / (x 10 ⁻⁴ g ml ⁻¹)	MG ⁺ / (x 10 ⁻⁴ g ml ⁻¹)	Mass concentration MG ⁻ /MG ⁺ (g ml ⁻¹)	pH			
				3	5	8	10
A	5.0	5.0	1.0	U	U	U	U
B	10.0	3.8	2.6	U	U	U	U
C	15.0	2.5	6.0	U	S	S	S
D	17.5	1.9	9.2	U	S	S	S
E	20.0	1.3	15.3	S	S	S	S
X	5.0	5.0	1.0	U	-	U	-
Y	12.5	3.1	4.0	U	-	U	-
Z	20.0	1.3	15.3	S	-	S	-

Based on Table 1, a phase diagram for mixed microgel stability (MM) at different mass concentrations ratio of MG^-/MG^+ as a function of pH had been plotted (Figure 6). A phase diagram should be able to explain the stability phases of MG^-/MG^+ at different composition as a function of pH. Therefore degree of freedom has been removed to simplify a triangular phase diagram into a two dimensional easy to interpret plot. Moreover this plot was ready to use as a comparison with published data^{7,11}. Results obtained were agreeable with the previous study reported by Snowden *et.al.*¹¹. As the mass concentration increased transformation occurred to the MM systems from unstable phase separated (white area) to stable and dispersed (yellow area). The aggregation behaviour was clearly affected by the relative concentration of the two oppositely charged microgel species.

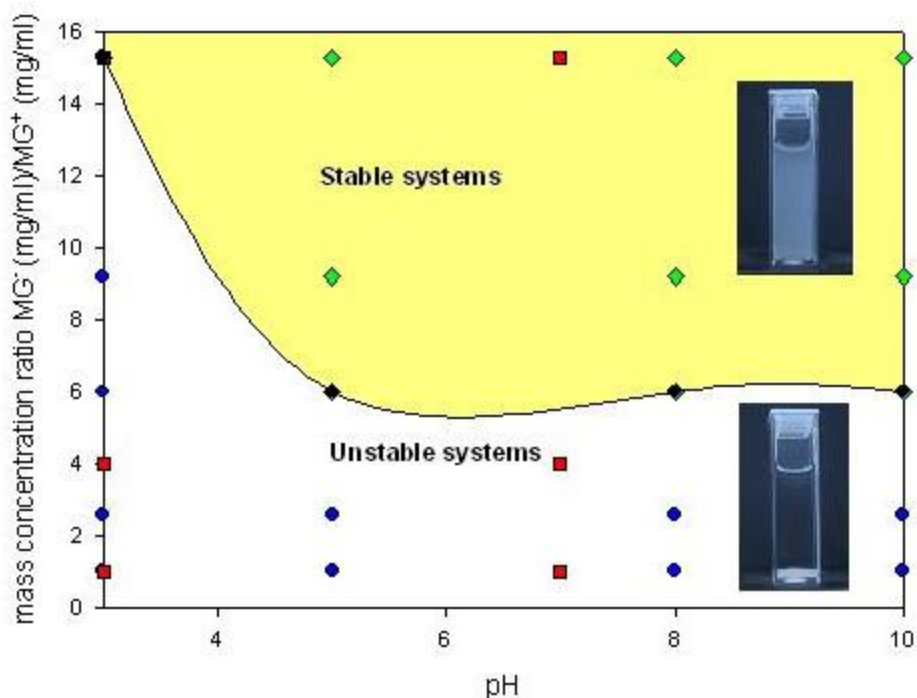


Figure 6: The phase diagram at 25°C for stable systems (green diamonds) and unstable systems (blue circles) compared to previous results reported by Snowden *et.al.*¹¹ (red squares). The new results were in good agreement with that previous study.

As can be seen, the phase diagram showed at pH 3 all samples were unstable^{7,11}. According to Stark *et.al.*⁷ the surface charge density increased due to pH adjustments. Opposite charges were neutralised resulting a domination of van der Waals attractive forces hence leading to system aggregation. In contrary, by raising the pH value, surface charge of mixed systems were also increased resulting re-stabilization of that systems. Although there was weak van der Waals attraction between oppositely charged microgel particles, however the steric repulsion was able to overcome these attractions.

The aggregation behaviour was also influenced by the relative concentration of MG^-/MG^+ . As the MG^- concentration increased, the transition could be seen from unstable system (below 6) to a stable system (above 6). The increasing of pH giving a rise to negatively charged density hence, a colloid stability was achieved by virtue of electrostatic repulsion between like-charged particles.

AuMES-NP-MM samples optimization

Based on Table 1, further investigations were made by adding a constant of AuMES-NPs ($0.04 \times 10^{-4} \text{ g ml}^{-1}$). Figure 7 shows the AuMES-NP-MM dispersions at pH 3 and pH 10 for the samples described in Table 1. At pH 3 samples A, B, C and D separated into two distinct phases with a lower turbid phase separating from a clear upper majority portion, taking up to 7 days to achieve final separation. Sample E remained as a stable dispersion at pH 3; a similar observation was reported by Snowden *et. al.*¹¹. Upon increasing pH to 10 only sample D and E that did not show flocculation. Based on the both results, only sample D gave a good reversible performance at pH 3 and 10. Therefore this formulation (sample D with formulation: $17.5 \times 10^{-4} \text{ g ml}^{-1} \text{ MG}^-$ and $1.9 \times 10^{-4} \text{ g ml}^{-1} \text{ MG}^+$) was chosen for further optimization, investigation and application.

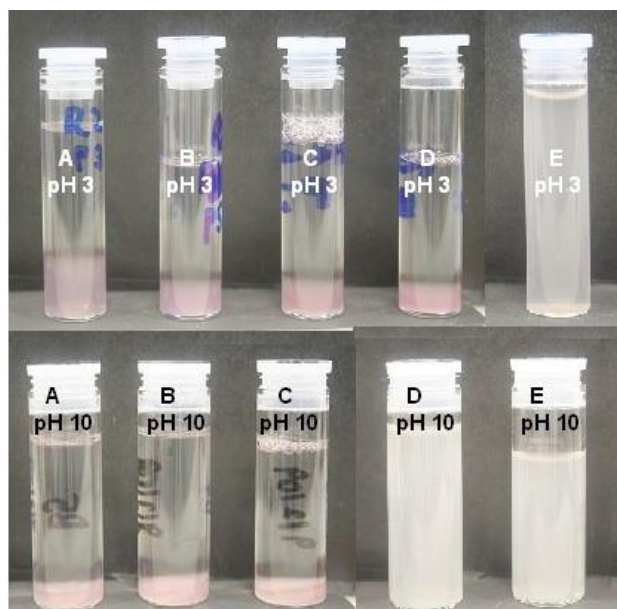


Figure 7: AuMES-NP-MM dispersion behavior with different relative ratios of microgel at pH 3, pH 5, pH 7 and pH 10.

Estimation of the number of AuMES-NPs per microgel particle

In previous sections it has been demonstrated that AuNPs were able to disperse in a mixed microgel systems. Moreover, the systems used were reversible and adjustable. Thus, to understand AuMES-microgel complexes systems, it is important to know of how much the AuNPs; i) dispersed in microgels ii) the formation which complex with microgels.

The number of AuMES-NPs per MG^+ microgel has been calculated. However a limitation was realised as it was not possible to know accurately the exact calculate polymer molecular weight. Therefore an approximation was used in this calculation. The assumptions were made:

- i) In the fully collapsed state, there was no solvent in the polymer microgel particles.
- ii) All monomers were transformed into monodisperse polymers.
- iii) Density of monomer and polymer are equal to 1 g cm^{-3} .
- iv) Assuming all Au^+ were reduced to Au^0 therefore the AuMES-NPs mass can be calculated.

The calculations were separated into two stages, firstly the number density of AuMES-NPs and secondly the number density of MG⁺ polymer particles. The calculations done were based on the final composition in the formulated mixtures being used. Where:

$$m_{\text{Au}} = \text{total mass of gold} = 1.65 \times 10^{-5} \text{ g cm}^{-3}.$$

$$m_{\text{mon}} = \text{total mass of monomer} = 8.03 \times 10^{-3} \text{ g cm}^{-3}.$$

i.e. the dilution factors from original gold and microgel stocks to generate the final mixture were already taken into account. The monomer was assumed to have an average molecular weight (mw) based on the ratio of NIPAM to 2VP = 3:1.

$$\text{Where } mw_{\text{mon}} = mw_{\text{PNIPAM}} + mw_{2\text{VP}} = 0.75 + 0.25$$

For calculations, the symbols used were: m (mass); ρ (density); V (volume); n (number of moles); Avogadro's number (N_A) = $6.023 \times 10^{23} \text{ mol}^{-1}$.

a) AuMES-NPs

The initial mass of gold in the final mixture was $1.65 \times 10^{-5} \text{ g cm}^{-3}$ and the density for gold bulk was 19.32 g cm^{-3} .

The volume for a gold particle where the average radius for gold used was 3.5nm (results shown in section 3.1.3:

$$\text{Equation 1} \quad V_{\text{Au}} = \frac{4\pi r^3}{3} = 1.79 \times 10^{-19} \text{ cm}^3$$

The mass of an individual particle may be estimated as:

$$\begin{aligned} \text{Equation 2} \quad m &= \rho V \\ &= 19.32 \text{ g cm}^{-3} \times 1.79 \times 10^{-19} \text{ cm}^3 \\ &= 3.47 \times 10^{-18} \text{ g} \end{aligned}$$

In order to know the number density of AuMES-NPs the bulk mass per particle of gold was divided by the mass of a single AuMES-NPs.

$$N_{\text{Au}} = \frac{1.65 \times 10^{-5} \text{ g cm}^{-3}}{3.47 \times 10^{-18} \text{ g}} = 4.75 \times 10^{12} \text{ cm}^{-3}$$

Therefore the number density of AuMES-NPs in 1 cm^3 is $4.75 \times 10^{12} \text{ cm}^{-3}$.

b) MG⁺ particles

The mass of monomer used in the final mixture was $8.03 \times 10^{-3} \text{ g cm}^{-3}$, the average mw of monomer (mw_{monomer}) 2VP used to prepare MG⁺ microgel ($105.14 \text{ g mol}^{-1}$). The density of the polymer was assumed as 1.0 g cm^{-3} .

Therefore, the molar volume (V) for monomer is $105.14 \text{ cm}^3 \cdot \text{mol}^{-1}$. Since the number of molecules in a mol is $6.023 \times 10^{23} \text{ molecules mol}^{-1}$, the volume for 1 monomer molecule (the molecular volume) is:

$$V_{\text{monomer}} = \frac{105.14 \text{ cm}^3 \text{ mol}^{-1}}{6.023 \times 10^{23} \text{ mol}^{-1}} = 1.75 \times 10^{-22} \text{ cm}^3$$

Assuming at the collapsed state of the MG there was no entrapped solvent, the average radius at this point was $1.5 \times 10^{-5} \text{ cm}$. Hence, for a spherical MG^+ microgel particle:

Equation 3
$$V_{\text{polymer}} = \frac{4\pi r^3}{3}$$

The value for V_{polymer} obtained was $1.41 \times 10^{-14} \text{ cm}^3$

Now we need to know number of monomers per polymer (N_{segment}):

Therefore
$$\begin{aligned} N_{\text{segment}} &= \frac{V_{\text{polymer}}}{V_{\text{monomer}}} \\ &= \frac{1.41 \times 10^{-14} \text{ cm}^3}{1.75 \times 10^{-22} \text{ cm}^3} \\ &= 8.10 \times 10^8 \text{ monomers per polymer} \end{aligned}$$

The molecular weight could be estimated by multiplying the monomer molecular weight ($\text{mw}_{\text{monomer}}$) with number of segments monomers per polymer:

$$\text{mw}_{\text{monomer}} \times N_{\text{segment}} = 105.14 \text{ g mol}^{-1} \times 8.1 \times 10^8$$

giving $8.50 \times 10^{10} \text{ g mol}^{-1}$. From this result the number density of polymers could be calculated:

$$\begin{aligned} n_{\text{MG}^+} &= \frac{\text{mass of monomer used}}{\text{molecular weight}} \\ &= \frac{8.03 \times 10^{-3} \text{ g cm}^{-3}}{8.50 \times 10^{10} \text{ g mol}^{-1}} \\ &= 9.41 \times 10^{-14} \text{ mol cm}^{-3} \text{ (moles of polymer per cm}^{-3}\text{)} \end{aligned}$$

Thus the number density of polymers could be obtained by multiplying by Avagadro's number, giving $5.70 \times 10^{10} \text{ cm}^{-3}$. Finally, the number of AuMES-NPs per MG^+ polymer molecule could be estimated as:

$$\begin{aligned} &\frac{N_{\text{Au}}}{N_{\text{MG}^+}} \\ &= \frac{4.75 \times 10^{12}}{5.70 \times 10^{10}} \\ &= 83 \end{aligned}$$

Another approach uses the average microgel radius of 1.50×10^{-5} cm; therefore the total of microgel surface area (S_{MG^+}) can be estimated:

$$\text{Equation 4} \quad S_{MG^+} = 4\pi r^2 = 2.81 \times 10^{-9} \text{ cm}^2$$

Imagine the AuMES-NPs were arranged in a close-pack array and curvature effects were ignored. Therefore, the total surface area of gold particles arranged in this way (diameter 7.0×10^{-7} cm):

$$\begin{aligned} S_{Au} &= r^2 \times \text{number of AuMES-NP} \\ &= 4.90 \times 10^{-13} \text{ cm}^2 \times 83 \\ &= 4.00 \times 10^{-11} \text{ cm}^2 \end{aligned}$$

Comparison of these surface areas show that total amount of area covered by AuMES-NPs was much less than that available on the surface of a single microgel particle. Thus this result supports the initial hypothesis that AuMES-NPs were randomly distributed on MG^+ microgel particles as reported previously.^[24]

Assuming the diameter of AuMES-NPs could not be smaller than 7 nm and were close-packing arrangement. Therefore, potentially gold particles could fit a microgel particle surface:

$$\begin{aligned} \frac{S_{MG^+}}{S_{Au}} &= \frac{2.81 \times 10^{-9} \text{ cm}^2}{4.09 \times 10^{-13} \text{ cm}^2} \\ &= 6845 \end{aligned}$$

This second calculation gave a broad idea of how many gold nanoparticles that could fit a single MG^+ particle. Approximately about 6845 gold nanoparticles could be fitted around if they were arranged in close-packed.^[22-24] In comparison with the current research, it showed that the experiment was handled in much diluted range of gold nanoparticles concentration.

Conclusion

This study has demonstrated that AuNPs well dispersed in mixed microgel systems. A stability test was conducted at room temperature and a phase diagram has been plotted. The results showed heteroaggregation behaviour for each sample was affected by the different concentration of oppositely charged microgels. Furthermore, in order to understand and determine AuNPs dispersion in the microgel systems, calculations were made based on several estimations. It was found that the AuMES-NPs were randomly distributed on MG^+ microgel particles which was significant with previously reported in the literature. The results confirmed that AuNPs were able to be dispersed in a mixed microgel systems. These interesting results giving a picture that MMS have a great potential to act as reusable catalyst supports, and may also be enhanced with different inorganic material. This system is found to be an environmentally and economically viable, potentially to be used as a tool for support and recovery media.

Acknowledgement

A.M.L. thanks the Ministry of Higher Education of Malaysian for the research grant UKM-GGPM-NBT-030-2011 and FRGS/1/2011/SG/UKM/02/25

Experimental section

All experiments utilised water which was purified using mili-Q water standard (PureLab, Elga), with resistivity of 18.2 M Ω cm. Dialysis tubing (Fisher) with a M_w cut-off of 12,000-14,000 Daltons was used for microgels purification. For all samples, pH was measured by using a waterproof pH meter (HI98127, pHep Hanna). For microgel synthesis, poly(N-isopropylacrylamide) and 2-vinylpyridine were used as received. The cross-linking monomers divinylbenzene (DVB, Aldrich, 80%) N,N-methylenebisacrylamide (BA, Aldrich, 99%), were used as received. The initiator used for anionic microgels was potassium persulfate (KPS), and for the cationic microgels was 2,2'-azobis(2-methylpropionamide) dihydrochloride (V50, Waco, 95%). Aqueous solutions of HCl and NaOH were used to adjust pH.

Microgel syntheses

Anionic and cationic PNIPAM based microgels

Both the anionic poly(N-isopropylacrylamide) (PNIPAM is referred to as MG^-) and cationic poly(NIPAM-co-2-vinylpyridine) (abbreviated MG^+) were synthesized by deploying methods of Snowden *et.al.*¹¹. MG^- was synthesized using the following reagents and quantities. In a reaction flask, 800 mL of purified water (PureLab, Elga) was added to 0.51 g of potassium persulfate initiator. Separately, 5.0 g of NIPAM and 0.51 g of cross-linking agent N,N-methylenebisacrylamide (BA) were dissolved in 200 mL of purified water (mili-Q). The dissolved reagents were added to the reaction flask and the polymerization reaction was set at 70 °C under an inert atmosphere.

MG^+ was prepared in a similar manner, briefly, 800 mL of purified water was purged with nitrogen for 30 minutes in a 1 L, five-neck round bottom flask fitted with a mechanical stirrer which operated at 150 rpm. 0.50 g cationic initiator 2,2'-azobis(2-methylpropionamide) dihydrochloride (V50, Waco) was then added to the reaction flask and stirred. 200 mL of purified water (mili-Q standard) (PureLab, Elga), 3.75 g of NIPAM and 0.55g of BA together with 1.25 g of 2-vinylpyridine (2VP) were added together in a beaker and stirred for 15 minutes. This solution was then added to the reaction vessel with the temperature raised to 70 °C. The polymerization reaction was left to proceed for 6 hours with continuous stirring (~150 rpm). The outcome of the dispersion was filtered through glass wool followed by extensive dialysis against mili-Q water for one week with two changes of water per day.

Gold sol synthesis

Methods described by Davies *et. al.*²⁰ to prepare the gold sol were followed. Two milliliters of an aqueous solution of $\text{HAuCl}_4 \cdot 3\text{H}_2\text{O}$ (2.5×10^{-4} M) was diluted to 180 mL water to result in a pale yellowish colour. Next, 20 mL of an aqueous sodium 2-mercaptoethanesulfonate (NaMES) solution (1×10^{-3} M) was added (stirring 700 rpm). Freshly dissolved sodium borohydride (NaBH_4) (at concentration of 7.9×10^{-2} M) in a minimum amount of water was added to the reaction mixture. A quick colour change from pale yellow to brown was observed, indicating the formation of gold nanoparticles.

Preparation of mixed microgel dispersions

The relative concentrations of the samples prepared are shown in Table 1. An extensive optimization process was carried out to identify this concentration (Table 2). The samples were made up in mili-Q water and pH was adjusted using small quantities of 1 M aqueous NaOH or HCl respectively. All samples were prepared according to the concentration ratio shown in Table 2. In general, the gold containing sample preparation involved a two-step process, firstly mixing AuMES-NP with MG^+ to form AuMES-NP- MG^+ , and secondly mixing AuMES-NP- MG^+ with MG^- to form AuMES-NP-MM.

Table 2: Composition of samples prepared

Sample / $\times 10^{-4}$ g/ml	MG^-	MG^+	AuMES- NP
MM	17.5	1.9	- 0.17
AuMES-NP- MG^+	-	8.3	
AuMES-NP-MM	17.5	1.9	0.04

References

- 1- Sanchez, J. M.; Hidalgo, M.; Salvada, V. *Solvent Extraction and Ion Exchange*, **2000**, *18*, 1199 - 1217.
- 2- Martínez, S.; Navarro, P.; Sastre, A. M.; Alguacil, F. J. *Hydrometallurgy*, **1996**, *43*, 1-12.
- 3- Akita, S.; Yang, L.; Takeuchi, H. *Hydrometallurgy*, **1996**, *43*, 37-46.
- 4- Myakonkaya, O.; Eastoe, J. *Advances in Colloid and Interface Science*, **2009**, *149*, 39-46.
- 5- Minati, L.; Biffis, A. *Chemical Communications*, **2005**, 1034-1036.
- 6- Yusa, S.-i.; Yamago, S.; Sugahara, M.; Morikawa, S.; Yamamoto, T.; Morishima, Y. *Macromolecules*, **2007**, *40*, 5907-5915.
- 7- Starck, P.; Ducker, W. A. *Langmuir*, **2009**, *25*, 2114-2120.
- 8- Fernandez-Nieves, A.; Marquez, M. *J. Chem. Phys.*, **2005**, *122*, 084702-084706.
- 9- Bradley, M.; Vincent, B.; Warren, N.; Eastoe, J.; Vesperinas, A. *Langmuir*, **2005**, *22*, 101-105.
- 10- Sawai, T.; Shinohara, H.; Ikariyama, Y.; Aizawa, M. *Journal of Electroanalytical Chemistry*, **1991**, *297*, 399-407.

- 11- Hall, R. J.; Pinkrah, V. T.; Chowdhry, B. Z.; Snowden, M. J. *Colloids and Surfaces A: Physicochemical and Engineering Aspects*, **2004**, 233, 25-38.
- 12- Wang, Q.; Heiskanen, K. *International Journal of Mineral Processing*, **1992**, 35, 121-131.
- 13- Morris, G. E.; Skinner, W. A.; Self, P. G.; Smart, R. S. C. *Colloids and Surfaces A: Physicochemical and Engineering Aspects*, **1999**, 155, 27-41.
- 14- Morris, G. E.; Vincent, B.; Snowden, M. J. *Journal of Colloid and Interface Science*, **1997**, 190, 198-205.
- 15- Hui, D.; Nawaz, M.; Morris, D. P.; Edwards, M. R.; Saunders, B. R. *Journal of Colloid and Interface Science*, **2008**, 324, 110-117.
- 16- Wang, C.; Flynn, N. T.; Langer, R. *Advanced Materials*, **2004**, 16, 1074.
- 17- Das, M.; Zhang, H.; Kumacheva, E. *Annual Review of Materials Research*, **2006**, 36, 117-142.
- 18- Wang, Y.; Wei, G.; Wen, F.; Zhang, X.; Zhang, W.; Shi, L. *Journal of Molecular Catalysis A: Chemical*, **2008**, 280, 1-6.
- 19- Karg, M.; Wellert, S.; Pastoriza-Santos, I.; Lapp, A.; Liz-Marzan, L. M.; Hellweg, T. *Physical Chemistry Chemical Physics*, **2008**, 10, 6708-6716.
- 20 -Davies, P. T.; Vincent, B. *Colloids and Surfaces A: Physicochemical and Engineering Aspects*, *In Press, Corrected Proof*. **2009**.
- 21- Pelton, R. H.; Chibante, P. *Colloids and Surfaces*, **1986**, 20, 247-256.
- 22- M. Bradley, B. Vincent, G. Burnett, *Langmuir*, **2007**, 23, 9237.
- 23- Lin, W.; Kobayashi, M.; Skarba, M.; Mu, C.; Galletto, P.; Borkovec, M. *Langmuir*, **2005**, 22, 1038-1047.